Journal of the European Ceramic Society xxx (2016) xxx–xxx

Contents lists available at www.sciencedirect.com

Journal of the European Ceramic Society

journal homepage: www.elsevier.com/locate/jeurceramsoc

Effects of phase constitution and microstructure on energy storage properties of barium strontium titanate ceramics

Yong Jun Wu[a,b,c], Yu Hui Huang[a,b,c], Nan Wang[a,b,c], Juan Li[d,*], Mao Seng Fu[e], Xiang Ming Chen[b]

[a] State Key Laboratory of Silicon Materials, Zhejiang University, Hangzhou 310027, China
[b] Laboratory of Dielectric Materials, School of Materials Science and Engineering, Zhejiang University, Hangzhou 310027, China
[c] Cyrus Tang Center for Sensor Materials and Applications, Zhejiang University, Hangzhou 310027, China
[d] College of Materials Science and Engineering, Zhejiang University of Technology, Hangzhou 310006, China
[e] School of Materials Science and Engineering, Northwestern Polytechnical University, Xi'an 710072, China

ARTICLE INFO

Article history:
Received 19 September 2016
Received in revised form
28 December 2016
Accepted 30 December 2016
Available online xxx

Keywords:
Barium strontium titanate
Microstructure
Spark plasma sintering
Energy storage

ABSTRACT

Barium strontium titanate ($Ba_{0.3}Sr_{0.7}TiO_3$, BST) ceramics have been prepared by conventional sintering (CS) and spark plasma sintering (SPS). The effects of phase constitution and microstructure on dielectric properties, electrical breakdown process and energy storage properties of the BST ceramics were investigated. The X-ray diffraction analysis and dielectric properties measurements showed that the cubic and tetragonal phase coexisted in the SPS sample while the CS sample contained only tetragonal phase. Much smaller grain size, lower porosity, fewer defects and dislocation were observed in SPS samples, which greatly improved the electrical breakdown strength of the $Ba_{0.3}Sr_{0.7}TiO_3$ ceramics. The enhanced breakdown strength of the SPS samples resulted in an improved maximum electrical energy storage density of 1.13 J/cm^3 which was twice as large as that of the CS sample (0.57 J/cm^3). Meanwhile, the energy storage efficiency was improved from 69.3% to 86.8% by using spark plasma sintering.

1. Introduction

Electric energy storage materials have been receiving much attention because they play a key role in efficient, clean and versatile use of energy [1]. In particular, while conventional batteries and solid oxide fuel cells offer higher energy density, capacitors possess higher power density and much faster charge and discharge rates [2]. This is essential for pulsed power applications and regenerative braking system [3,4]. In order to meet the increasing need for improving the mass- and volume-efficiency of energy storage components, the energy density of capacitors must be increased [5]. At least two approaches are utilized to address this issue. One is the use of supercapacitors based on electrolytic solution and the other is the use of solid state capacitors based on dielectrics [3,6]. Various materials such as oxides, glass and polymers have been extensively investigated to optimize them as candidates for high energy density dielectrics [7–13]. Generally, the involved dielectrics are focused on linear dielectrics, ferroelectrics and antiferroelectrics. The energy storage density J is described by [14]

$$J = \int_0^E E\mathrm{d}P = \int_0^E \varepsilon_0\varepsilon_r(E)E\mathrm{d}E \quad (1)$$

where J is the energy storage density (J/m^3), E is the applied electric field (V/m), ε_0 is the permittivity of free space (8.854×10^{-12} F/m), dP is the change in polarization induced in the dielectric by the applied field and $\varepsilon_r(E)$ is the electric-field-dependent permittivity ($\varepsilon_r(E) = \varepsilon(E)/\varepsilon_0$). For linear dielectrics, the permittivity is not electric-field-dependent and the energy storage density can be derived as

$$J = \frac{1}{2}\varepsilon_0\varepsilon_r E^2 \quad (2)$$

As can be seen from these equations, to store more energy in a dielectric, a high permittivity (high ε_r) and a high breakdown strength allowing the application of high E are required.

High energy storage density can be achieved in some linear dielectrics, such as mica, glass, diamond-like carbon films and several polymer films [2,9–13]. These materials exhibit high breakdown strength, but suffer from low dielectric constant. Ceramics,

* Corresponding author.
E-mail addresses: juanli@zjut.edu.cn, wutiger74@yahoo.com (J. Li).

http://dx.doi.org/10.1016/j.jeurceramsoc.2016.12.052
0955-2219/

on the other hand, have high/giant dielectric constant, but are limited to relatively low breakdown strength [14,15]. Over years, a lot of research has been focused on improving breakdown strength of linear dielectric ceramics for high energy density storage. The $Ba_{1-x}Sr_xTiO_3$ (BST) is one of the most popular materials because of its excellent dielectric properties and the ability to engineer different dielectric behavior by mixing with other components or forming composite structure. Glass and/or oxides, such as Al_2O_3 and MgO, have been adopted to refine the microstructure of BST materials and thus increase the breakdown strength [16–18].

In the past decades, spark plasma sintering, which allows for quick densification has been found to be a useful and efficient method in tailoring the microstructure of ceramics [19–21]. The advantages of SPS method, such as low sintering temperature, short sintering time and microscopic electrical discharges between particles, make it suitable to control the grain size and grain boundary of ceramics and to tailor the configuration and interface of composites [22–24].

In this paper, barium strontium titanate ceramics were prepared and the effects of phase constitution and microstructure on dielectric properties, electrical breakdown process and electrical energy storage properties of BST ceramics were investigated in detail.

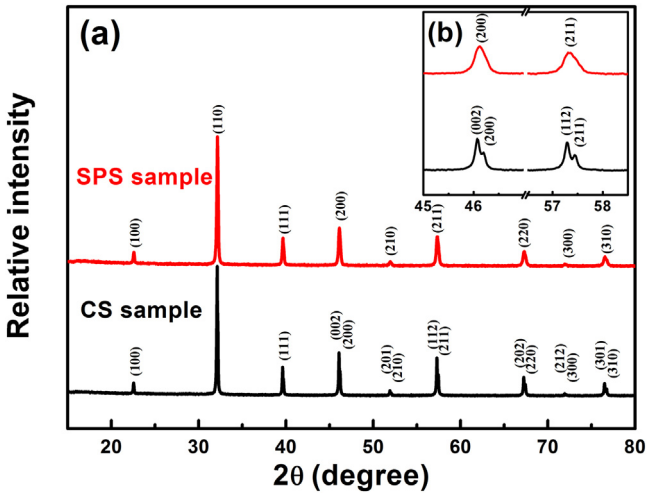

Fig. 1. (a) XRD patterns of $Ba_{0.3}Sr_{0.7}TiO_3$ ceramics prepared by conventional sintering and spark plasma sintering. (b) Enlargement of diffraction peaks at (2, 0, 0) and (2, 1, 1) crystallographic plane.

2. Experimental procedure

$Ba_{0.3}Sr_{0.7}TiO_3$ powders were synthesized by the conventional solid state reaction method. Stoichiometric mixtures of $SrCO_3$ (>99.95%, Aladdin), $BaCO_3$ (>99.99%, Shanghai Chemical Reagent) and TiO_2 (>99.99%, Shanghai Chemical Reagent) were ball milled with zirconia balls in distilled water for 24 h and calcined at 1150 °C in air for 3 h. To prepare $Ba_{0.3}Sr_{0.7}TiO_3$ ceramics by the conventional sintering method (CS), the calcined powders were mixed with a poly(vinylalacohol) binder solution and uniaxially pressed into disk samples with a diameter of 12.5 mm. After removal of the binder, the green disks were sintered at 1400 °C for 3 h in an alumina crucible, and were called CM samples. To prepare $Ba_{0.3}Sr_{0.7}TiO_3$ ceramics by SPS, the calcined powders were placed in a graphite die and sintered at 1000 °C for 5 min under a vacuum of 6 Pa with an SPS apparatus (SPS-1050, SPS Syntex Inc., Kanagawa, Japan). During the period of heating, a pressure of 30 MPa was applied to the sample. The heating rate was 100 °C/min from room temperature to 900 °C, 40 °C/min from 900 °C to 980 °C, and 20 °C/min from 980 °C to 1000 °C. All the spark plasma sintered samples were polished and thermally treated at 1000 °C for 2 h in air and were called SPS samples. Both the CS samples and the SPS samples were then polished and coated on each major face with Au electrodes.

The crystalline phases of sintered samples were characterized by X-ray diffraction (XRD, D/MAX 2550/PC, Rigaku, Tokyo, Japan) using Cu K_α radiation. The microstructures were observed from the thermally etched surfaces with field emission scanning electron microscopy (SEM, S-4800, Hitachi, Tokyo, Japan). The grain size of the sintered samples was determined from the SEM micrographs using the linear intercept method. The samples for transmission electron microscopy were prepared via the ultrasonic cutting of disks 3 mm in diameter and mechanical polishing to a thickness of about 100 μm. The central portions of the disks were reduced further to about 10 μm by mechanical dimpling (Model656, Gatan, SanFrancisco, CA, USA) followed by final polishing. The final perforation of the BST sample was conducted via precision argon-ion milling (Model691, Gatan, San Francisco, CA, USA), using an acceleration voltage of 4 kV. The TEM images were obtained at 300 kV by a transmission electron microscope (TEM, Tecnai F30G2, FEI, Hillsboro, OR, USA).

The dielectric properties were evaluated with a broadband dielectric spectrometer (Turnkey Concept 80, Novocontrol Technologies GmbH & Co. KG, Hundsangen, Germany) in a broad range of temperature (140–400 K) and frequency (100 Hz–1 MHz) with a heating rate of 2 K/min. A ferroelectric test system (Premier II, Radiant Tech. Inc., NM, USA) were used for *P-E* loops measurement. The energy storage densities and efficiencies were calculated from the *P-E* loops.

3. Results and discussion

3.1. Phase constitution and microstructure observation

Fig. 1 shows the XRD patterns of the CS sample and SPS sample. All the diffraction peaks for both samples can be indexed. As shown in Fig. 1(b), the split of diffraction peaks at high angles corresponding to the tetragonal phase are only found in the CS sample. The XRD analysis indicates that the CS sample consists of only the tetragonal BST phase, while a high content of the cubic BST phase exists in the SPS sample. The cubic BST phase in the SPS sample may present linear dielectric properties, which is beneficial for the reduction of remnant polarization and the improvement of the energy storage efficiency.

SEM micrographs on the thermally etched surfaces and fracture surfaces of the CS sample and SPS sample are shown in Fig. 2. The CS sample exhibits inhomogeneous microstructures where some pores can be discerned from the thermally etched surfaces. In contrast, the SPS sample presents a uniform, fine and dense microstructure where the average grain size is 880 nm. As shown in Fig. 2(b) and (d), clear grain boundaries can be observed in the SPS sample, whereas they are hard to distinguish in the CS sample. This indicates different fracture mechanisms in these two samples: transcrystalline fracture in the CS sample due to abnormal grain growth and intergranular fracture in the SPS sample. Fig. 3(a) and (b) show the TEM micrographs of the $Ba_{0.3}Sr_{0.7}TiO_3$ ceramics prepared by the conventional method and spark plasma sintering, respectively. It can be observed that there are fewer dislocations and defects in the SPS sample. Previous studies reported that a high concentration of dislocations in ceramics may lead to the possibility of coalescence and the formation of cracks under very strong electric fields [25]. Therefore, fewer dislocations in the SPS sample may contribute to the enhanced breakdown strength.

Please cite this article in press as: Y.J. Wu, et al., Effects of phase constitution and microstructure on energy storage properties of barium strontium titanate ceramics, *J Eur Ceram Soc* (2016), http://dx.doi.org/10.1016/j.jeurceramsoc.2016.12.052